ENGINEERING RESEARCH JOURNAL (ERJ)

Vol. 1, No. 49 Jul. 2021, pp 145-162

Journal Homepage: http://erj.bu.edu.eg

Study on Hydrodynamic Performance of Unsymmetrical Double Vertical Slotted Barriers

Karim Badr Hussein and Mohamed Ibrahim

Lecturer of Irrigation and Hydraulics, Faculty of Engineering, Al-Azhar University

Abstract. The main objective of the breakwater systems is to protect the closed water yard from waves and storms, as they help bring calm inside the port and thus achieve safety for ships inside it, and ease of operation. This paper presents the results of the study on wave interaction with vertical slotted water breakers. The research was conducted on two breakwater models, each of which was defined as follows: The first breakwater has two perforated walls: the lower portion is porous, while the top part is solid, while the second wall is the polar opposite of the first, with a porosity of 50% in both. The second breakwater is similar to the first, but it lacks the horizontal slit wall. The first and second breakwaters were compared, and the result indicate that the first breakwater hydrodynamic output performance the second in the range (10-15 %).The second breakwater is affected by the wave force less in the range (85-90%) than its breaker first counterpart. On the models that have been tested, the wave's force increases as its relative length (h/L) increases. According to the results of this study, the transmission factor (kt) rises as the relative length (h / L) decreases, while the reflection factor (kr) decreases as the relative length (h / L) reduces. FLOW-3D has the ability to calculate the velocities in front and behind the breakwaters and can be used in similar studies.

Keywords : Coastal, Breakwater, FLOW-3D, Perforated Wall, Energy Dissipation.

1. INTRODUCTION

The coastal area is considered one of the most important and vital areas in any country. But some natural phenomena such as waves, coastal currents and tides affect the stability of this region in the form of erosion of the shoreline and changes in the bottom. Therefore, coastal protection facilities play a significant part in protecting the coastal area and restoring its balance [2, 3]. Breakwaters are facilities built inside the sea, either parallel to the shore line or connected to the shore in order to reduce the energy of the waves arriving to the shore, thus protecting the shore from erosion as a result of wave attacks or for the purpose of determining the water area of the port and protecting it from waves and currents and thus the ships are safely docked to complete the shipping and dispatching operations [8, 20]. Conventional breakwaters consist of huge formations of reinforced concrete or rocks that extend from the sea floor to the surface - and thus unlikely to be used in deep waters and form solid and permanent structures. The benefit of overcoming these limits with flexible and affordable solutions has prompted INGEMAR since 1980 to seek solutions using facilities that are more efficient and reliable than ever before. Breakwaters come in a variety of shapes, materials, and performance levels, including visible, floating, and submerged barriers. The visible bulkheads, which are known as traditional barriers, have high efficiency, but they distort the aesthetic view of the beach [14, 21]. They require many construction materials and the cost of construction is high. On the other hand, floating barriers require less construction materials and their construction cost is lower, but their efficiency is relatively small. Hence,

submerged partitions are considered to be one of the best alternatives because they avoid the drawbacks of these types [18].

Submerged barriers are one of the most important installations to protect beaches, and one of the advantages of submerged barriers is that the cost of their construction is relatively small in relation to the visible barriers, and allow the passage of water from front to back, allowing water to regenerate behind the barrier [6,15] . Also, it does not distort the aesthetic view of the beach, does not obstruct the view, and has a relatively small effect on the neighboring beaches. However, the subsidence of submerged dikes after construction reduces their efficiency in dispersing wave energy and protecting shorelines. The high water level also affects the efficiency of the barrier [19]. Therefore, improving the efficiency of submerged breakwaters is one of the most important points in the field of coastal protection.

Many papers, periodicals, and articles on breakwaters were gathered, studied, and reviewed, revealing that many scientists were focused on creating new types of economic wave barriers.

The aim of this study is to numerically model and evaluate the hydrodynamic efficiency of a well-developed breakwater. This paper was also compared to similar studies in the field, as well as the hy second models.This is presented in this paper under the following headlines:

- Materials and methods.
- Results and discussion.
- Conclusions.

2. MATERIALS AND METHODS

2.1 The Proposed Innovative Model

Fig 1 and 2 illustrate two economic breakwaters that were proposed. It's a permeable breakwater made up of two vertically perforated walls that are similar. The first wall is porous in the upper level, while the second wall is porous in the lower level. A permeable part's porosity is equal to 50%.
The difference between the first and second perforated walls was 0.5 meters, as determined by the depth of the water. Model No. 1 was a perpendicularly pierced breakwater with a horizontal cut wall, while model no. 2 was a perpendicularly pierced wall breakwater without a horizontal cut wall.

2.2 Numerical Molding

The suggested breakwater was numerically simulated in this paper using FLOW-3D. FLOW-3D is a popular the computational Fluid Dynamics (CFD) programme that offers valuable insights into many physical flow processes. It solves the three-dimensional Navier-Stokes and continuity equations in an ordered, rectangular grid. The general mass continuity equations used by FLOW-3D for three-dimensional incompressible flows are summarized in the Equations below. It is worth noting that (CFD) applications are commonly used in all engineering disciplines, especially marine and coastal engineering. **Fig**. 3 and 4 represent a set of robust sub elements in the model. The computational model in FLOW-3D has the advantage of meeting engineering and hydraulic boundary conditions [5, 17].
FLOW-3D was used to apply the model and create many scenarios for numerical simulation of the proposed breakwater. Two independent grids of varying cell sizes were used in this model to strike a convenient compromise between precision/accuracy and measuring time [4]. Mesh cells for low frequency waves are 1 cm in diameter in each direction, while mesh cells for high frequency waves are 0.5 cm in diameter in each direction. To avoid any recoveries, whether from the end of the channel or the wave paddle, it is critical to determine the time window for analyzing the wave height according to the wavelength [16, 24]. Calculating the height of the incident spectrum's reflected and transmitted waves is important. As a result, the reflection factor "kr" is calculated using the wave profiles obtained from

$$: kr = \frac{Hr}{Hi} \qquad (1)$$

Where: Hr is reflected wave height and Hi is incident wave height.

The transmission factor" kt" was determined from the wave transmission profile by using given equation:

$$kt = \frac{Ht}{Hi} \qquad (2)$$

Where: Ht is the height of the wave that is being transmitted [23].

The factor of energy dissipation "kd" can be calculated using the above equations and the following relationship:

$$kd = 1 - kr^2 - kt^2 \quad (3)$$

2.3 Analytical Study

The potential velocity `"Φ" is believed to be a cyclic motion in period T and can be written as:

$$\Phi(x,z,t) = \mathrm{Re}\ \frac{-igh_i}{2\omega}\phi(x,z)\frac{1}{\cosh\ kh}e^{-i\omega t} \quad (4)$$

Where Re is a part of a complex value's real value, h is depth of water;

ω is wave angular frequency, g is acceleration due to gravity, $i = \sqrt{-1}$ and K is wave number (K=2π/L).

The dispersion relationship can be expressed as follows $\omega = gk\tanh(Kh)$

$$\frac{\partial\phi_1(x)}{\partial x} = \frac{\partial\phi_2(x)}{\partial x} = iG^{-}(\phi_1(x) - \phi_2(x))$$

at $x = -a$ for $-h \le z \le -D1$ (5)

$$\frac{\partial\phi_2(x)}{\partial x} = \frac{\partial\phi_3(x)}{\partial x} = iG^{-}(\phi_2(x) - \phi_3(x))$$

at $x = a$ for $-D2 \le z \le 0$ (6)

The proportional constant $G^{-} = \frac{G}{b}$, the permeability parameter, G, is defined as:

$$G = \frac{\varepsilon}{f - is} \quad (7)$$

Where ε is the porosity of the structure is determined by the pile dimensions and spacing, f is The friction factor and S is the inertia coefficient equal to:

$$s = 1 + cm\left(\frac{1-\varepsilon}{\varepsilon}\right) \quad (8)$$

Where *cm is a mass* coefficient that has been applied. The velocity potential was solved in an infinite number of ways as follows [10]:

$$\phi_1(x) = \phi_i + \sum_{m=0}^{\infty} A_{1m}\cos[\mu_m(h+z)]\exp(\mu_m(x+a))$$

at $x \le -a$ (9)

$$\phi_2(x) = \sum_{m=0}^{\infty} A_{2m}\cos[\mu_m(h+z)]\exp(-\mu_m(x+a)) + \sum_{m=0}^{\infty} A_{3m}\cos[\mu_m(h+z)]\exp(\mu_m(x-a))$$

At $-a \le x \le a$ (10)

and

$$\phi_3(x) = \sum_{m=0}^{\infty} A_{4m}\cos[\mu_m(h+z)]\exp(-\mu_m(x-a))$$

At $x \ge a$ (11)

The coefficients A_{1m}, A_{2m}, A_{3m} and A_{4m} might be computed by utilizing the matching criteria (i.e. adding(9),(10), and(11) with (4) as well as (5) the matrix formula at the breakwater:

$$\begin{bmatrix} \sum_{m=0}^{\infty} C_{11}^{(mn)} & \sum_{m=0}^{\infty} C_{12}^{(mn)} & \sum_{m=0}^{\infty} C_{13}^{(mn)} & \sum_{m=0}^{\infty} C_{14}^{(mn)} \\ \sum_{m=0}^{\infty} C_{21}^{(mn)} & \sum_{m=0}^{\infty} C_{22}^{(mn)} & \sum_{m=0}^{\infty} C_{23}^{(mn)} & \sum_{m=0}^{\infty} C_{24}^{(mn)} \\ \sum_{m=0}^{\infty} C_{31}^{(mn)} & \sum_{m=0}^{\infty} C_{32}^{(mn)} & \sum_{m=0}^{\infty} C_{33}^{(mn)} & \sum_{m=0}^{\infty} C_{34}^{(mn)} \\ \sum_{m=0}^{\infty} C_{41}^{(mn)} & \sum_{m=0}^{\infty} C_{42}^{(mn)} & \sum_{m=0}^{\infty} C_{43}^{(mn)} & \sum_{m=0}^{\infty} C_{44}^{(mn)} \end{bmatrix} \begin{bmatrix} A_{1m} \\ A_{2m} \\ A_{3m} \\ A_{4m} \end{bmatrix} = \begin{bmatrix} b_{1n} \\ b_{2n} \\ b_{3n} \\ b_{4n} \end{bmatrix}$$

For n=1 , 2, 3 …….. ∞ (12)

Numerical methods may be used to solve equation (10). As a result, kr and kt were obtained;

$$kr = \left| A_{10} \right|$$

$$kt = \left| A_{40} \right|$$

Equation (3) can be used to compute the energy dissipation coefficient [11, 12].

2.4 Hydrodynamic Force

The hydrodynamic force is one of the important parameters in this study. The hydrodynamic pressure (p) can be expressed using Bernoulli's modified linear as shown below [1] :

$$p = -\rho\left(\frac{\partial \phi}{\partial t}\right)_{x=-a} = i\omega\rho(\phi_1 - \phi_2)_{x=-a} \quad (13)$$

$$p = -\rho\left(\frac{\partial \phi}{\partial t}\right)_{x=a} = i\omega\rho(\phi_2 - \phi_3)_{x=a}$$

x = a (14)

$$p = \frac{-\rho g H_i}{2}\frac{\cosh k(z+h)}{\cosh kh}(1 + k_r - k_t) \quad (15)$$

Following the determination of the hydrodynamic pressure (p), the hydrodynamic forces (F *) occurring on the breakwater can be calculated using the formulas below [7,22] :

$$F^* = \int_{-d}^{0} p(0,z)dz \quad (16)$$

$$F^* = -\frac{\rho g H_i}{2k}(1 + k_r - k_t)\tanh kh \quad (17)$$

$$F = \mathrm{Re}[F^* e^{-i\omega t}] \quad (18)$$

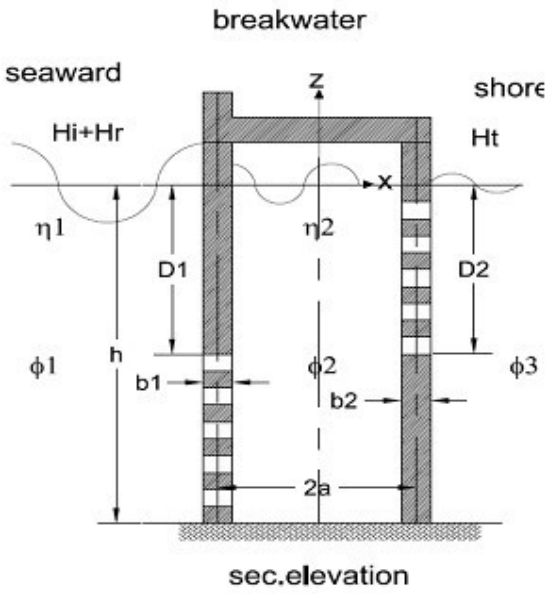

Fig.1- Breakwater with vertical porous wall and horizontal opening

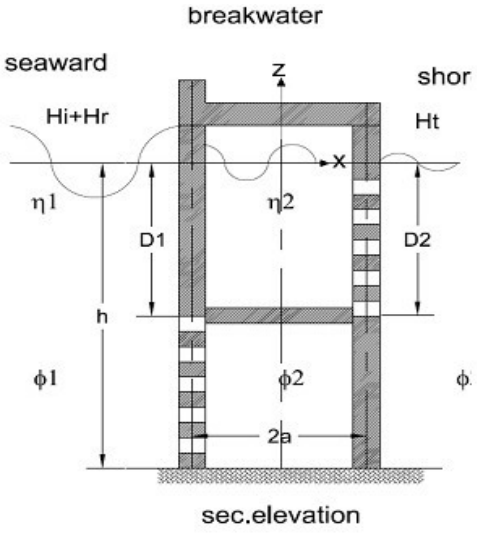

Fig.2 - Breakwater with vertical porous wall but no horizontal opening

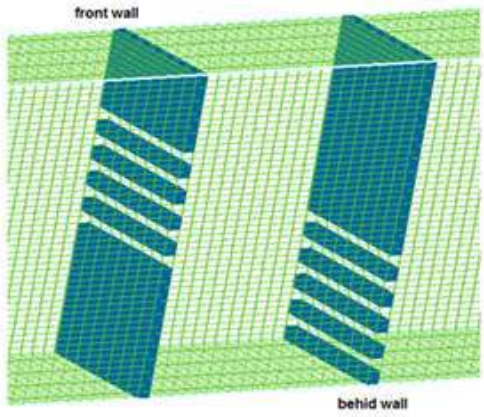

Fig.3 -Model of a breakwater without a horizontal opening

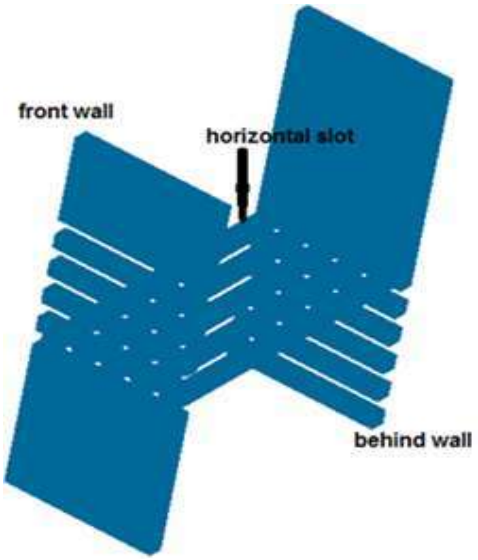

Fig.4 - Breakwater model with a horizontal opening

2.5 The Wave Channel

The experimental investigation was carried out by the wave channel. The channel was rectangular in shape, measuring 12 m by 2.0 m by 1.2 m (length, width, and depth). The gravel wave absorber was situated in the exit region and has a 3:1 slope to absorb the transmitted waves. The channel's walls were composed of reinforced concrete. The channel has an inlet zone, main zone, (working section) and outlet zone, **Photo** 1.

Photo .1 - The Wave Channel

3. RESULTS AND DISCUSSION

The hydrodynamic efficiency of the two forms of breakwaters was investigated and assessed using numerical models in this paper. The breakwater consists of two vertically porous walls, one with a horizontal opening and the other without. The upper portion of the first wall was impermeable, while the lower portion was permeable. Penetration in the upper part of the second wall was strong, while penetration in the lower part was weak. This research looked into propagation coefficients, reflection, and wave energy dissipation. The experiments were carried

out in the hydraulic laboratory of Zagazig University's faculty of engineering in Egypt, and the results were presented in **Table** .1 The experiment was conducted without the planned breakwater in order to assess impact wave height and time.

Table.1- The experimental results of the study

Different factors	Various Ranges						
Wave of occurrences (cm)	6.6	7.5	8.15	9.05	10.5	11.55	12.45
Wave duration (Sec)	1.45	1.37	1.29	1.18	1.12	0.98	0.91
Water depth(m)	0.4	0.4	0.4	0.4	0.4	0.4	0.4
Wave length(m)	2.40	2.29	2.15	1.89	1.70	1.45	1.19
width (2a)	0.2	0.2	0.2	0.2	0.2	0.2	0.2

Fig 6 illustrates the wave height obtained from a laboratory experiment performed at various frequencies without the use of a breakwater. **Fig** 7 clearly indicates that as the relative depth (h/L) increases, the transion coefficient (kt) decreases. The first and second water breaks were compared, and the findings revealed that the first water break's energy dissipation coefficient beats the second in the range of about (10-15 %). **Fig** 8 compares the results of this analysis for hydrodynamic parameters to those of Ji and Suh (2010),who used double perforated walls with no horizontal opening under the same conditions as a function of d/L, in this case D/d , B/d , ε and f were (0.5 - 1 - 0.5 – 1) respectively [9]. **Fig** 9 compares the effects of this study for hydrodynamic parameters to those of Laju et al. (2011) in this case D/d , B/d , ε and f were (0.35 – 0. 5 - 0.25 – 1.2) respectively.

Fig 10 shows Kt and kr for Comparison between Flolw-3D (without horizontal openings) and results from Laju et al. (2011) in this case D/d , B/d , ε and f were (0.35 – 0.5 - 0.25 – 1.2) respectively[13] .

As seen in **Fig** 11, the wave force has a larger effect on the first model than on the second. It can also be shown that the difference between the two models increase as relative depth increases.

The model (FLOW-3D) and the positions of the measuring probes are seen in **Fig** 12. **Fig** 13 shows the surface level at 0.9 and 1.1 seconds of wave duration after 2.0 m from the breakwater using (FLOW -3D) (T). **Fig** 14 illustrates the surface level at 1.5 seconds of wave duration, wave transmission at probe (1), and wave reflecting at probe (2).

Fig 15 displays vector and velocity domain for a single ring computed with FLOW- 3 D for time increases of 0.1 second and a wave frequency of 1 Hz. Higher speeds were found at the top of the wave and along the vents.

By studying the aforementioned figures, one can notice that the higher speeds are at the bottom of the openings that happens as a result of the impact of the obstacle. The speeds in front of the breakwater are very high, on the contrary, behind the breakwater is very low.

From the results of this study it was found that the flow between the breakwaters in the event of turbulence except for the field around the holes, the water is moving vertically.

Two experiments were used to investigate the influence of form and chamber width in velocity distribution fields with a constant porosity of 50% and a D/h of 0.5. In the first experiment, the average velocity field was shown in the area of the double punched breakwater with horizontal holes in two different states for B / h, which were 0.5 and 1 during the tenth wave cycle, as shown in **Fig** 16. With regard to the area of impermeable barriers, it is clear that the maximum velocities were 72.9 cm / s, seen **Fig** 16. The average velocity range is offered for porosity 0.50 porous baffles. The recycled area this time is very clear under the first breakwater versus the second one was blurred. On the breakwater surface, the contact of the water mass with the vacuoles is illustrated. At the same condition, maximum velocity for B/h=1.0 was 56.7 cm/s, which was higher than velocity for B/h=0.5, **Fig** 17.

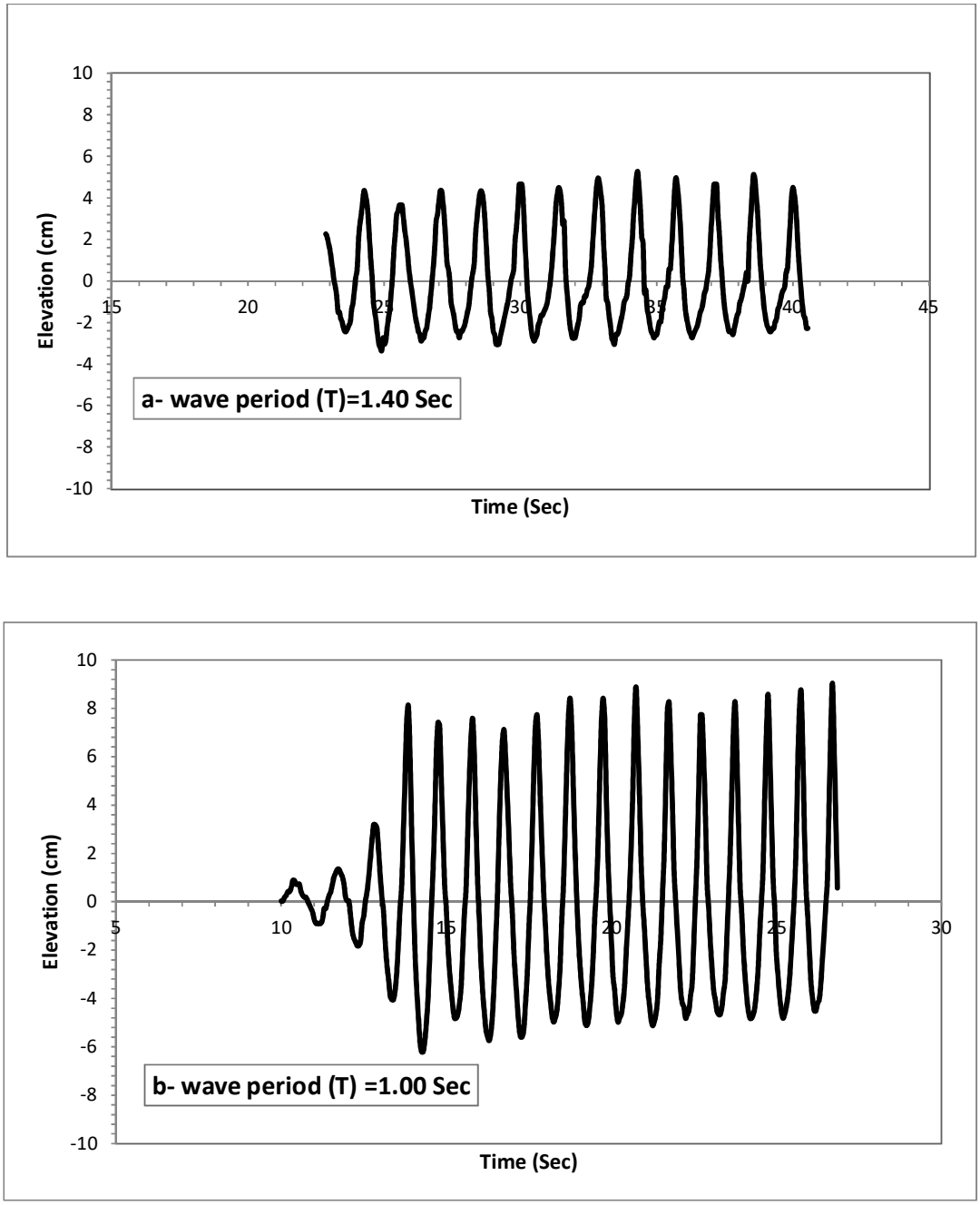

Fig.6 - Profiles of wave for different periods

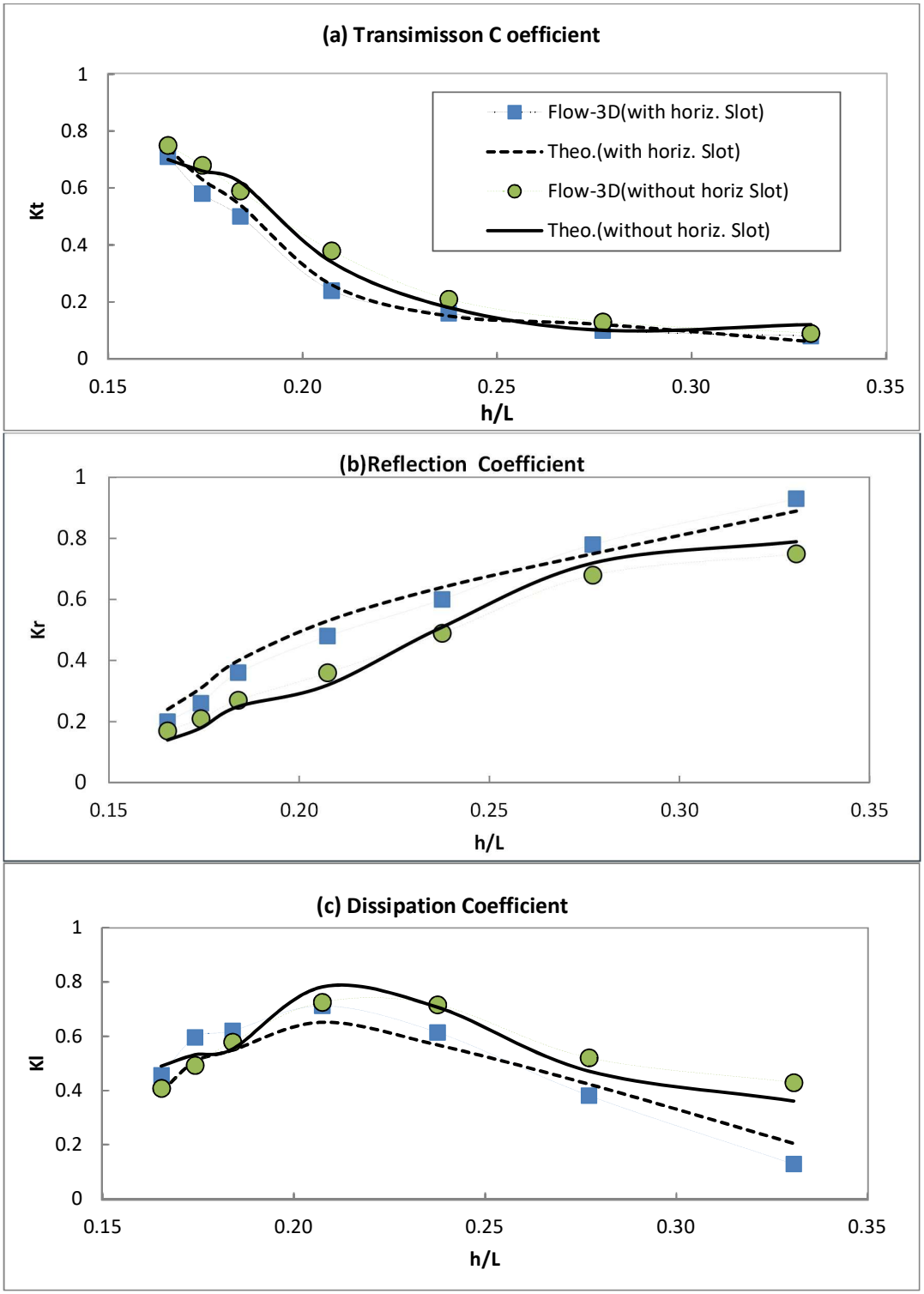

Fig. 7- kt, kr and kd for Comparison between (FLOW-3D) and The breakwater (with and without horizontal openings) at 2a and ε were (0.5h , 50%) respectively.

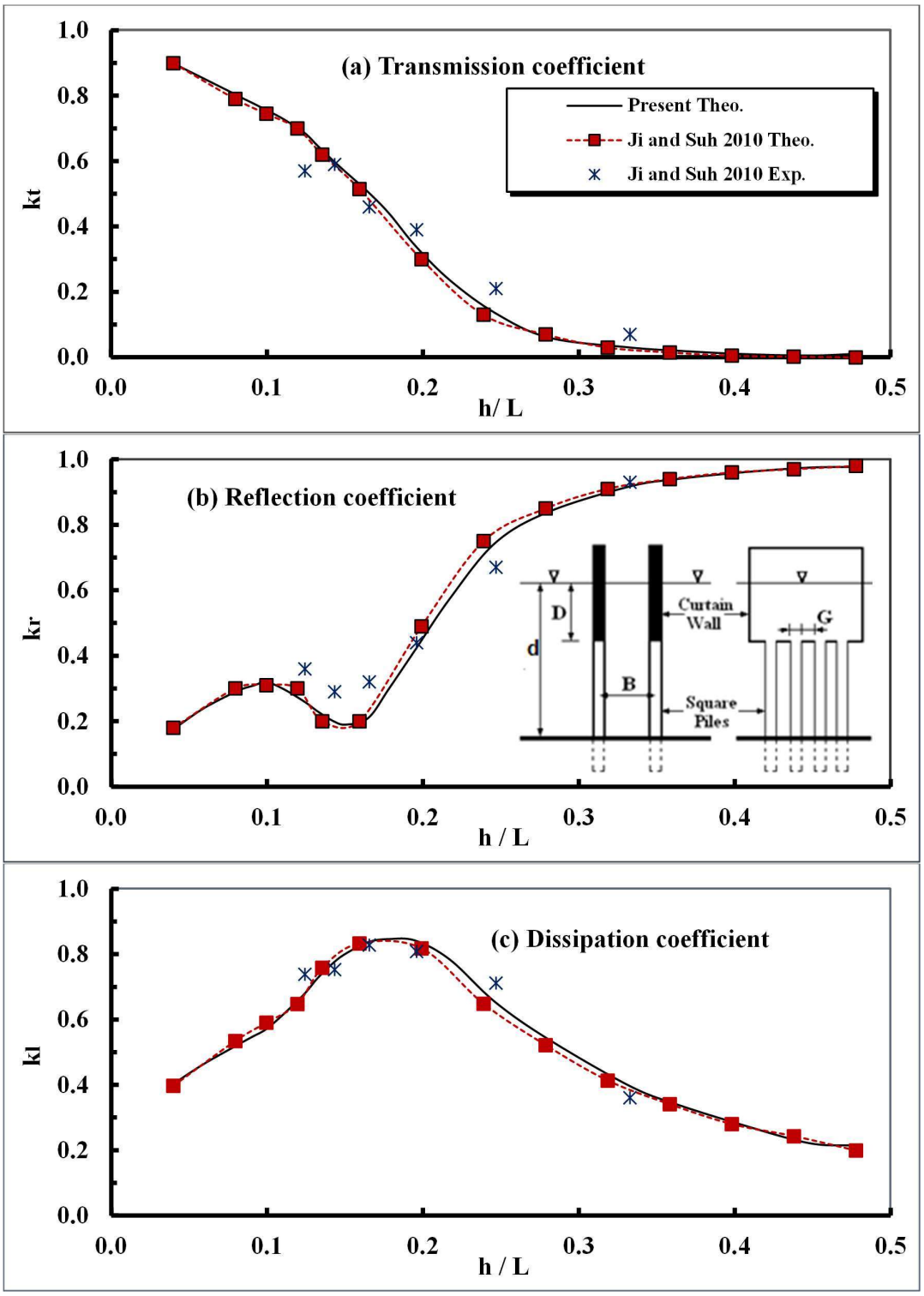

Fig. 8 - kt, kr and kd for Comparison between breakwater (without horizontal slots) and results from Ji and Suh (2010) at D/d = 0.5, B/d = 1, ε = 0.5, f = 2.

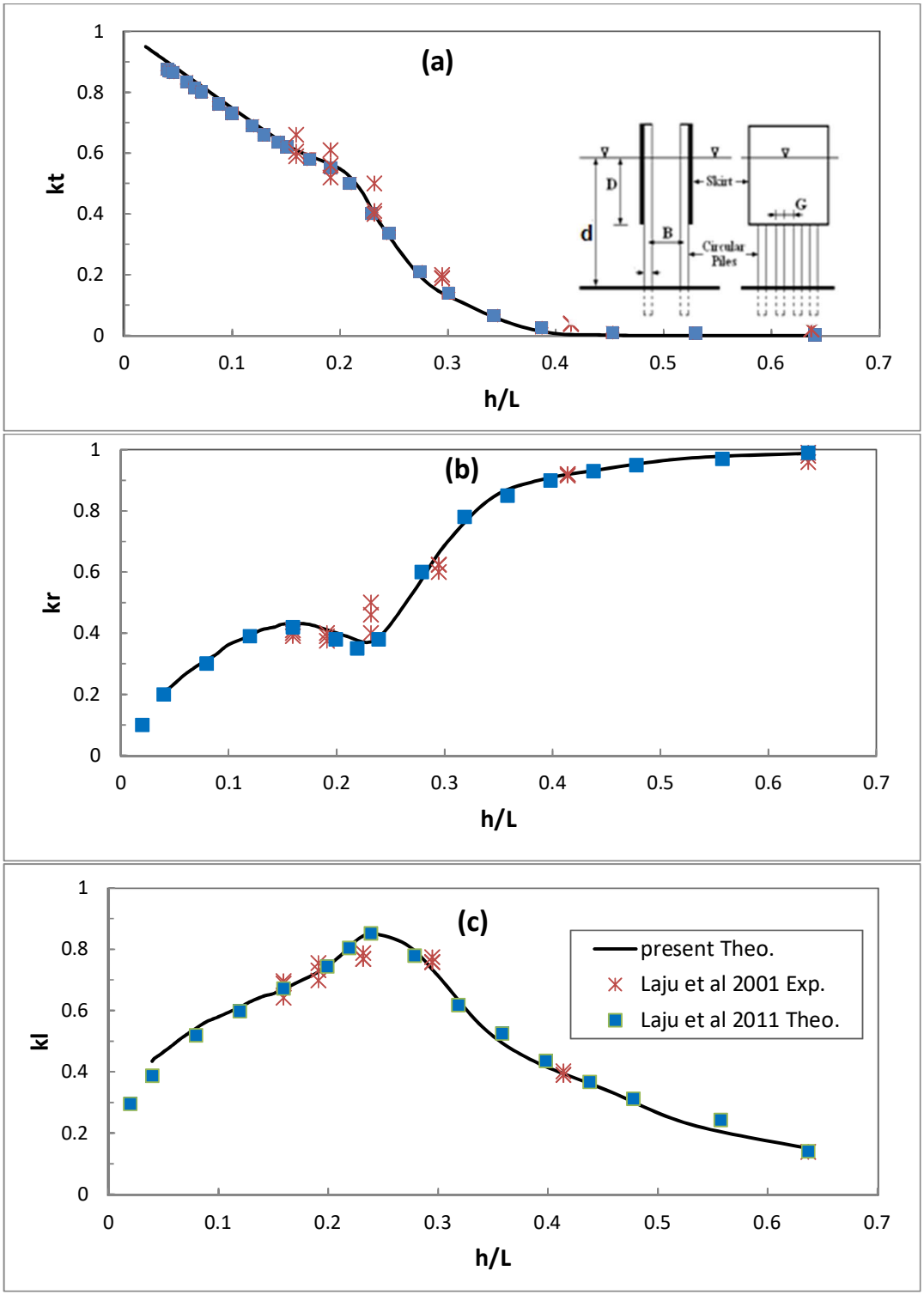

Fig. 9 - kt, kr and kd for Comparison between breakwater (without horizontal slots) and results from Laju et al. (2011) (at D/d, B/d, ε and f (0.35, 0.5,0.25 and1.2) respectively

.

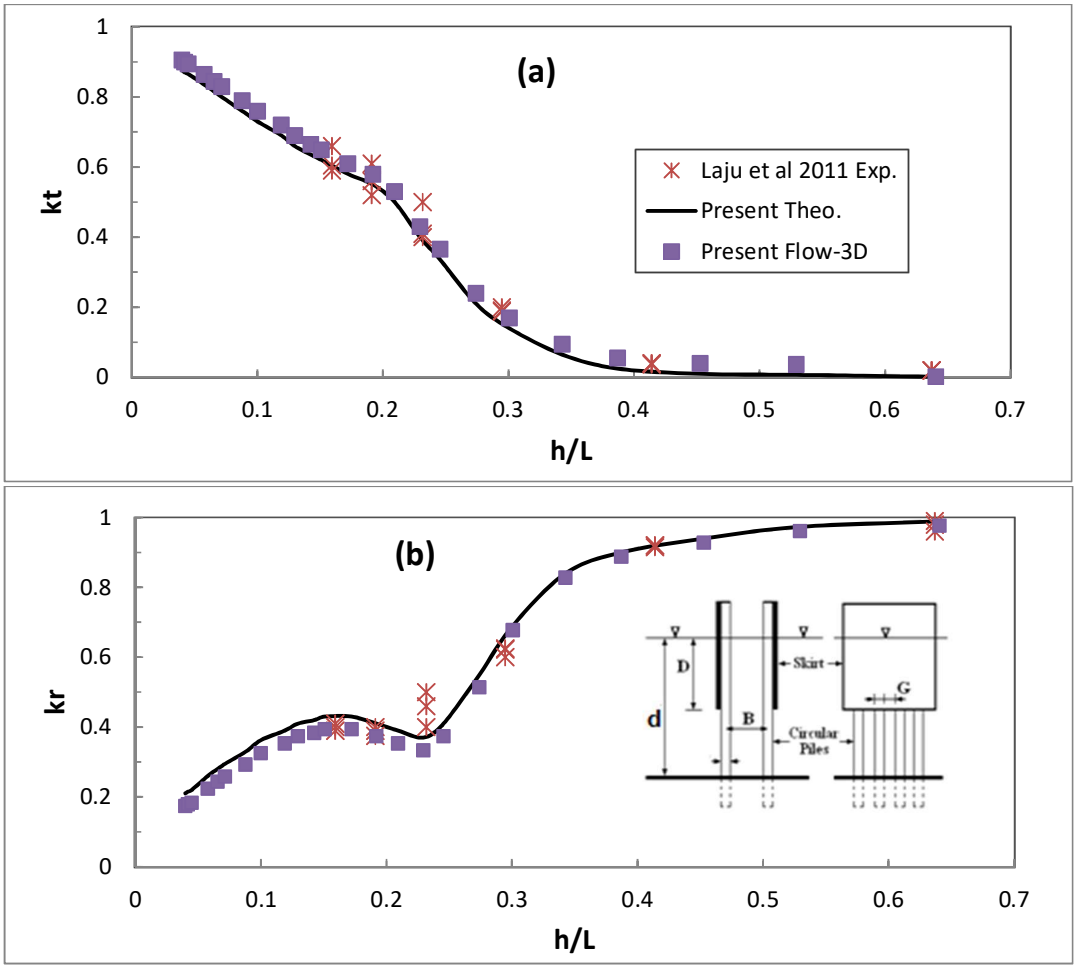

Fig. 10 - Kt and kr for Comparison between Flolw-3D (without horizontal slots) and results from Laju et al. (2011) at D/d, B/d, ε and f were (0.35, 0.5,0.25 and1.2) respectively.

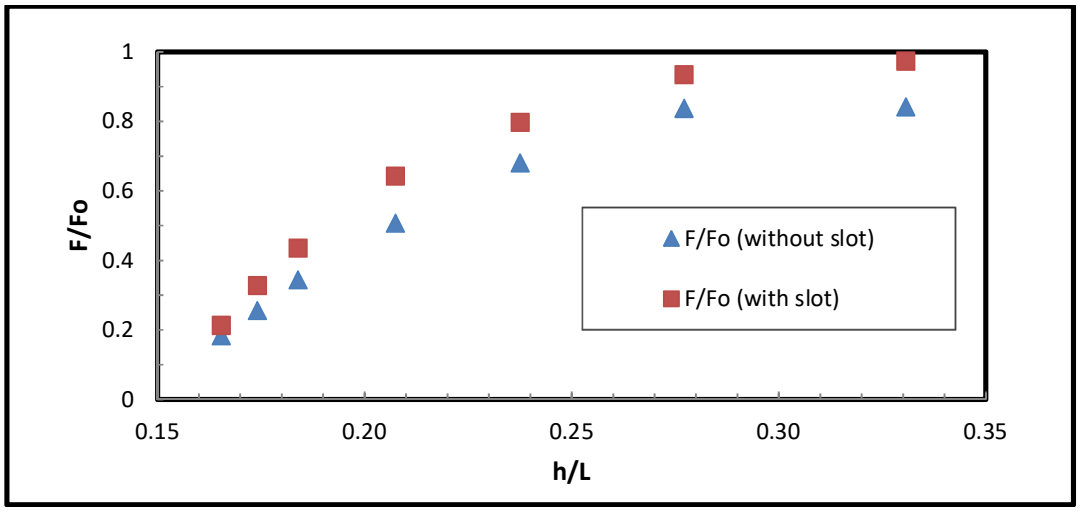

Fig. 11- Comparison between F/F_o (without slot) and between F/F_o (with slot) at $2\lambda = 0.5d$ and $\varepsilon = 0.5$

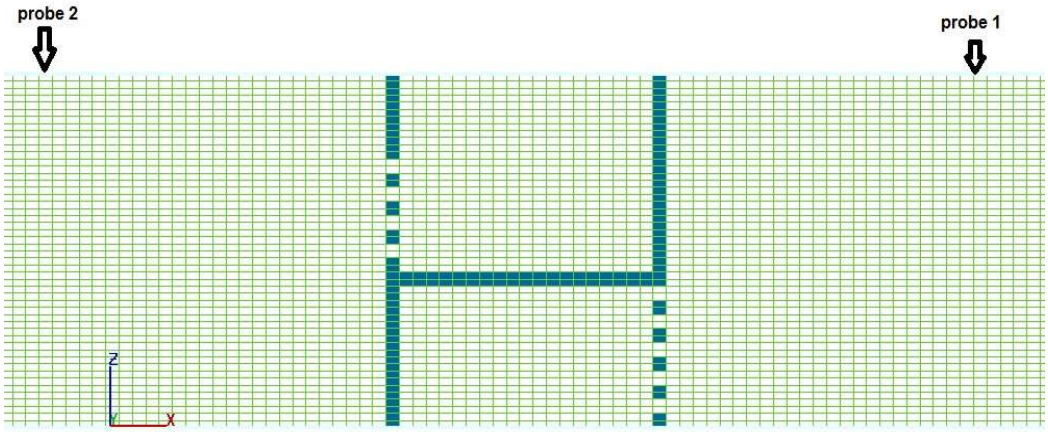

Fig. 12- Path of the wave, position of the wave reflection, and wave transmission

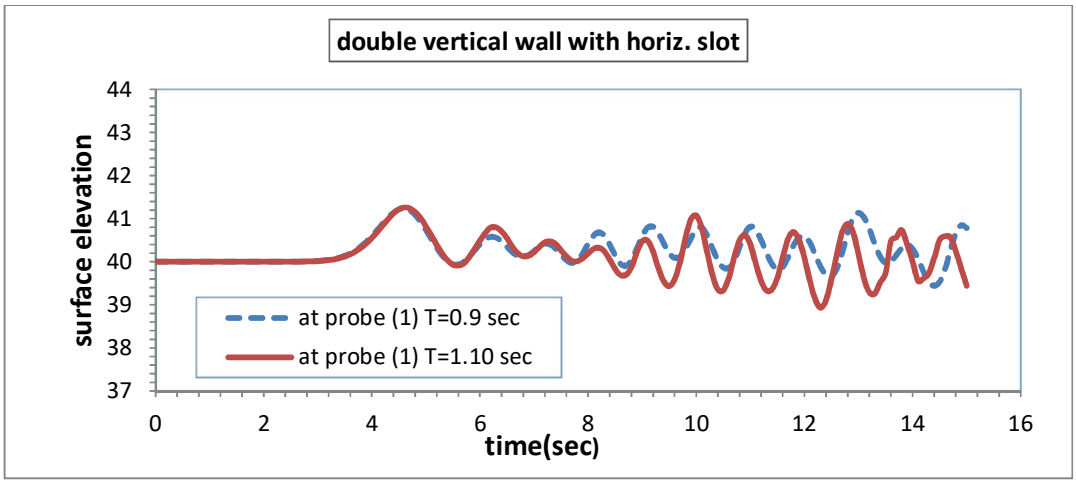

Fig. 13 - Change Surface height (cm) with time

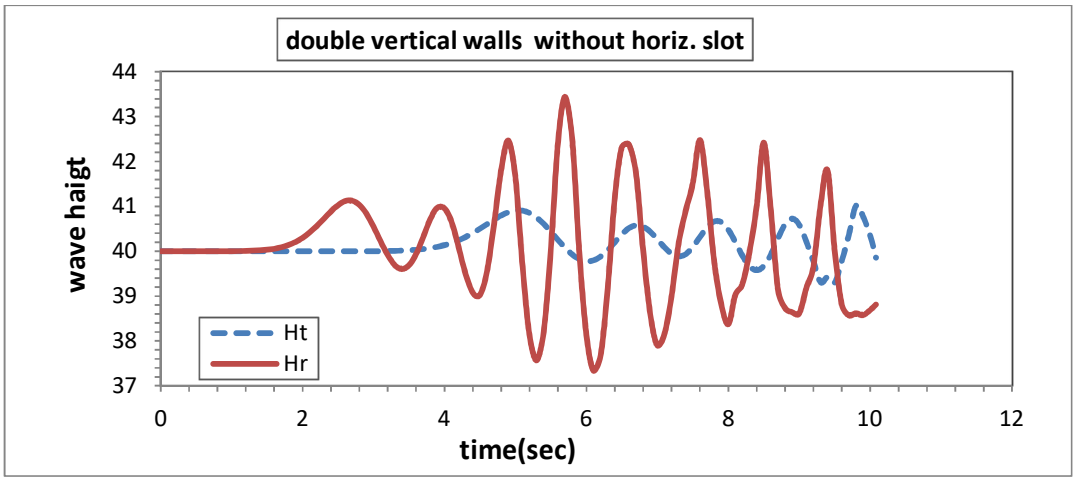

Fig. 14 - The surface level at 1.5 seconds of wave duration, wave transmission at probe (1), and wave reflecting at probe (2).

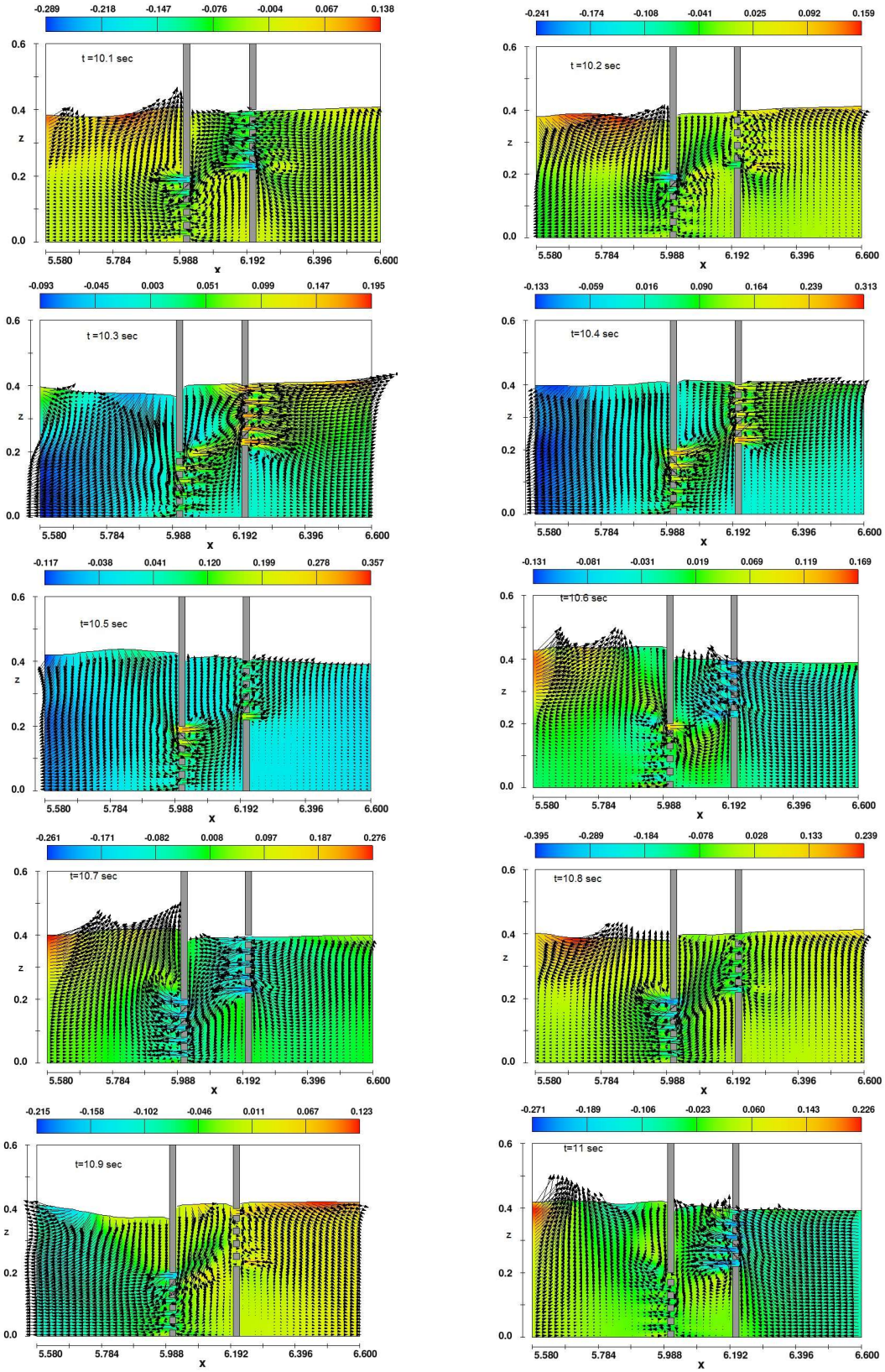

Fig. **15** - FLOW-3D results for velocity and velocity path at T, Hi, *dt* and 2a/*h* were (1.2 sec, 9 cm,0.1 sec and0.5) respectively

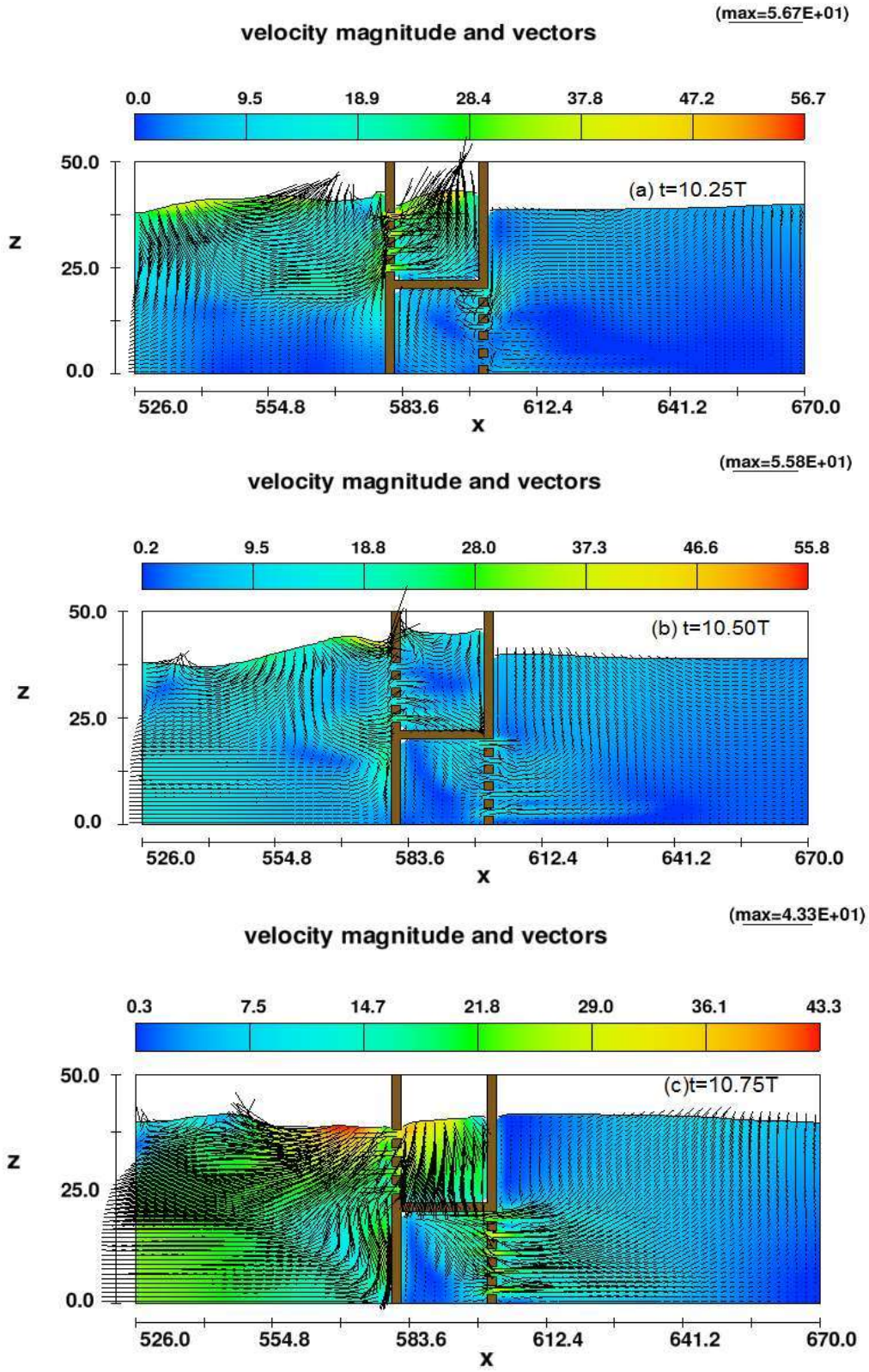

Fig.16 -Velocity in breakwater zone for ε, B/d, Hi and T were (0. 50, 0.5 , 9 cm and 1.2sec) respectively.

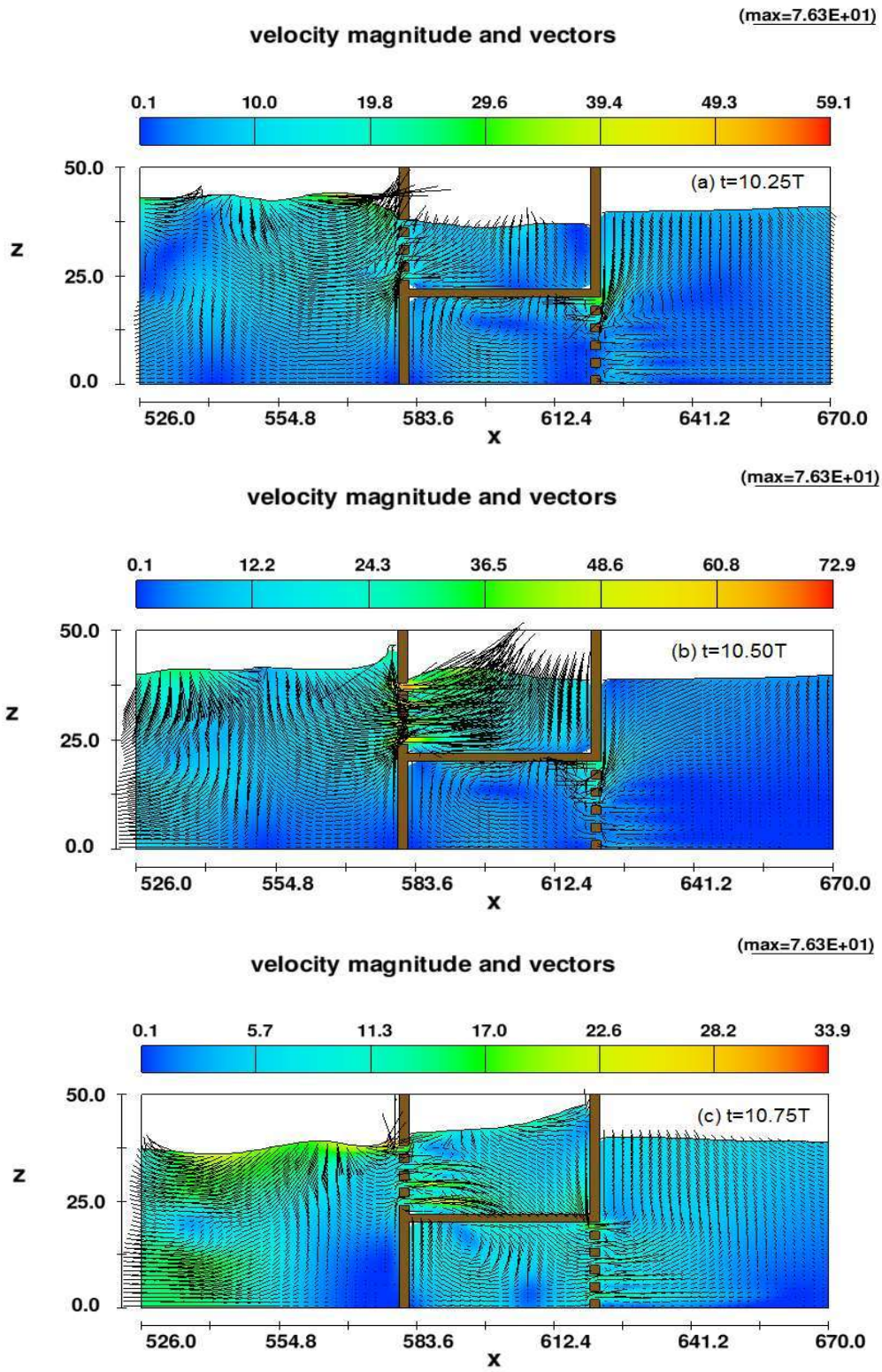

Fig. 17 -Velocity in breakwater zone for ε, B/d, Hi and T were (0. 50, 1, 9 cm and 1.2sec) respectively.

4. CONCLUSIONS

From the previous analysis of the obtained results, the conclusions which have been reached are as follow:

- Breakwaters are mechanically shaped and closely studied, according to the literature analyzed, but computational simulation has some contradictions. The Flow 3-D model was found to be capable of modeling the indicated breakwater among the models investigated.
- Experimental investigations and a computational model were used to verify Flow-3D.
- From the results and their analysis, it was found that Flow -3D has a high ability to characterize the interaction of the wave with a linear wave with perforated walls of the double vertical type. It's also able to reproduce the most critical characteristics of laboratory data and semi-analytical performance. The numerical results obtained by Flow -3D are perfectly satisfactory.
- The force of the wave on the models that have been studied is noticed that it increases with the increase in its relative length (h/L).
- The first model was affected more than the second model by the wave force in the range (10-15%).
- According to the results of this study, the transmission factor (kt) rises as the relative length (h / L) decreases, while the reflection factor (kr) decreases as the relative length (h / L) reduces..
- In a comparison of the first and second models, it is obvious that the first model's energy dissipation coefficient is higher than the second in the region of (10-15 percent).
- The second model outperforms previous comparable research in terms of hydrodynamic performance (3-7 percent).
- FLOW-3D has the ability to calculate the velocities in front and behind the breakwaters and can be used in similar studies.
- The magnitude of velocity for B/h=1.0 is greater than the magnitude of velocity for B/h=0.5 under the same conditions.

NOTATIONS

In this paper, the following symbols were used:

- A_{10} = factor of dynamic reflection;
- A_{40} = factor of dynamic transmitting;
- A_{1n} = complex unknown factors;
- λ = the half-way point between both the two walls;
- b = thickness of the vertical wall;
- C_m = factor of mass applied;
- f = friction factor;
- G = parameter permeation;
- g = Gravitational acceleration;
- h_i = height of the event wave;
- h_r = height of mirrored waves;
- H_t = height of the wave that was transmitted;
- h = depth of water;
- k = wave sum of the event;
- k_l = factor of energy dissipation;
- k_r = factor of reflection;
- k_t = factor of transmitting;;
- L = length of wave;
- T = duration of the wave;
- t = time;
- **x , z** = axis in two dimensions;
- ε_1 = porosity of the first wall's bottom section;
- ϕ_p = possibility for overall flow velocity;
- ϕ_1 = possibility for seaward velocity;
- ϕ_2 = Between the two walls, there is a possibility for velocity.;
- ϕ_3 = possibility for shoreward velocity and
- F* = force of the waves**.**

REFERENCE

[1] Ahmed, H., 2011. "Wave Interaction with Vertical Perforated wallsas a Permeable Breakwater," PhD. Thesis, Hydro Sciences (IGAW), Bergische University of Wuppertal, Germany, 2011.

[2] Hayashi, T., & Kano, T., 1966. "Hydraulic research on the closely space Pile breakwater." 10th Coastal Eng. Conf., ASCE, New York, Vol. 11, Chapter 50.

[3] Herbich, J. B., 1989. "Wave transmission through a double-row Pile breakwater." Proc. 21st Int. Conf. on Coastal Eng., ASCE, Chapter 165, Torremolinos, Spain.

[4] Hirt, C. W. and Nichols, B. D., 1981. "Volume of Fluid (VOF) method for the dynamics of free boundaries," J. Computat. Phys., vol. 39, no. 1, pp. 201-225.

[5] Hsu, H-H. & Wu, Y-C., 1999. "Numerical solution for the second-order wave interaction with porous structures." International Journal for Numerical Methods in Fluids, Vol. 29 Issue 3, pp. 265-288.

[6] Huang, C. J.; Chang, H. H.; and Hwung, H. H., 2003. "Structural permeability effects on the interaction of a solitary wave and a submerged breakwater," Coastal Engineering. Vol. 49, pp. 1-24.

[7] Isaacson, M.; Baldwin, J.; Premasiri, S. and Yang, G., 1999. "Wave interaction with double Perforatedbarrier,"Applied ocean research, Vol. 21, pp. 81-91.

[8] Isaacson, M.; Premasiri, S. and Yang, G., 1998. "Wave interaction with vertical Perforatedbarrier," J. of Waterway, Port, Coastal and Ocean Engineering, vol. 124, no. 3, pp. 118-125.

[9] Ji, C.H. and Suh, K.D. (2010) "Wave interactions with multiple-row curtainwall-pile breakwaters" J.Coastal Engineering vol. 57 issue 5, p. 500-512.

[10] Karim, M. F.; Tanimoto, K. and Hieu, P. D., 2009 "Modelling and simulation of wave transformation in porous structures

using VOF based two-phase flow model," Applied Mathematical Modellin. vo 33, pp. 343–360.

[11] Koraim, A. S.; Heikal; E. M. and Rageh,O. S., 2011. "Hydrodynamic characteristics of double permeable reakwater undregular waves," Coastal Eng., vol. 24, pp. pp.503–527.

[12] Koraim, A. S; Iskander, M. M. and Elsayed, W. R., 2014. "Hydrodynamic performance odouble rows of piles suspending horizontal c shaped bars," Coastal Eng., vol. 84, pp. 81–96.

[13] Laju, K., Sundar, V. & Sundaravadivelu, R., 2011. "Studies on Pile supported double skirt breakwater models." Journal of Ocean Technology, Vol. 2, No.1. pp. 32-53.

[14] Laju, K., Sundar, V. & Sundaravadivelu, R., 2011. "Hydrodynamic characteristics of pile supported skirt breakwater models." Journal of Ocean Re, 33,12-22.

[15] Lara, J.; Garcia, LN. and Losada, I.J., 2006. "RANS modelling applied to random wave interaction with submerged permeable structures," Coastal Engineering, vol. 53, pp. 395–417.

[16] Lara, J.L.; Losada, I.J. and .Guanche, R., 2008. "Wave interaction with low-mound breakwaters using a RANS model," Ocean Engineering, vol. 35, pp. 1388– 1400.

[17] Lin, P.; and Karunarathna, .S.A., 2007. "Numerical stud of solitary wave interaction with porous breakwaters," J. of waterway, port, coastal and ocean engineering. , pp. 352-363.

[18] Mansard, E .P. D. & Funke, E. R., 1980. "The measurement of incident and reflected spectra using a least squares method." In Proc. 17th Coastal Eng. Conf., Sydney, Australia, pp 159-174.

[19] Rageh, O.S.; Koraim, A.S., 2010. "Hydraulic performance of vertical walls with horizontal sloed as breakwater," Coastal Engineering , vol. 57, pp. 745–756, 2010.

[20] Sollit, C. K. & Cross, R.H., 1972. "Wave transmission through permeable breakwaters." Proceedings of the 13th Coastal Eng. Conf., ASCE, Vancouver, pp. 1827-1846.

[21] Suh, K. D., Shin, S. & Cox, D. T., 2006. "Hydrodynamic characteristics of Pile-Supported vertical wall breakwaters." J. of Waterways, Port, Coastal and Ocean Engineering, Vol.132, No.2, pp.83-96.

[22] Suh, K.D., Park, W.S., 1995. Wave reflection from perforated-wall caisson breakwaters. Coastal Engineering 26, 177-193.Suh, K-D., Park, J.K., Park, W.S., 2006. Wave reflection from partially perforated-wall caisson breakwater. Coastal Engineering 33, 264-280.

[23] Wiegel, R. L., 1960. "Transmission of wave past a rigid vertical thin barrier" J. Waterway, Port, Coastal and Ocean Eng., ASCE, Vol. 86, No.1.

[24] Yu, X., 1995. "Diffraction of water waves by porous breakwater.", J. of Waterway, Port, Coastal and Ocean Engineering, Vol. 121, No. 6, pp. 275-282.